Analyst

Accepted Manuscript

ROYAL SOCIETY OF CHEMISTRY

www.rsc.org/analyst

Measuring Masses of Large Biomolecules and Bioparticles Using Mass Spectrometric Techniques

Wen-Ping Peng*, Szu-Wei Chou, Avinash A. Patil

Department of Physics, National Dong Hwa University, Shoufeng, Hualien, 97401, Taiwan, R.O.C.

* To whom correspondence should be addressed, e-mail: pengw@mail.ndhu.edu.tw

Contract/grant sponsor: NSC 102-2112-M-259 -003 -MY3
Prepared for the Analyst (review article)

Keywords: large protein complexes, bioparticles, ion source, mass analyzer, detectors, mass measurement, mass assignment, mass resolution

Abstract

Large biomolecules and bioparticles play a vital role in biology, chemistry, biomedical science, and physics. Mass is a critical parameter for characterization of large biomolecules and bioparticles. To achieve mass analysis, choosing a suitable ion source is the first step and the instruments of detecting ions, mass analyzers and detectors, should also be considered. Abundant mass spectrometric techniques have been proposed to determine the masses of large biomolecules and bioparticles, and these techniques can be divided into two categories: The first category is to measure the mass (or size) of intact particles, including single particle quadrupole ion trap mass spectrometry, cell mass spectrometry, charge detection mass spectrometry, and differential mobility mass analysis; the second category aims to measure the mass and tandem mass of biomolecular ions, including quadrupole ion trap mass spectrometry, time-of-flight mass spectrometry, quadrupole orthogonal time-of-flight mass spectrometry and orbitrap mass spectrometry. Moreover, algorithms for mass and stoichiometry assignment of electrospray mass spectra are developed to obtain accurate structure information and subunit combinations.

1. Introduction

Mass spectrometric techniques can be applied to acquire masses and fragment of large biomolecules and of bioparticles which facilitate the study of biological process, interaction of biomolecules, and their structures and functions.[1-3] The size of large biomolecules and bioparticles are in the range from 1 nm to 100 μm. Those large biomolecules and bioparticles include protein complexes, viruses, bacteria and cells. So far, it is still a challenge to detect bioparticles with sizes from 20 nm to 100 nm.[4, 5] Many research groups have tried to develop mass spectrometers to detect the masses of these sizes. In general, a mass spectrometer includes an ion source, a mass analyzer and a detector and therefore selecting ion sources and designing workable mass analyzers and detectors are a necessity.[6]

Ions are a primary issue for mass analysis. The ion sources used in mass spectrometry (MS) for large ions include electrospray ionization (ESI)[7], matrix-assisted laser desorption/ionization (MALDI)[8, 9] and laser-induced acoustic desorption (LIAD)[10-12]. With ESI ion source, proteins, protein complexes and viral capsids are generated in air and kept intact in vacuum.[13-17] ESI ion source can produce multiple charged ions with mass-to-charge ratio (m/z) below 100000. However, when the particle size becomes large, particles gain higher charges on the surfaces (typically > 50+) and cause highly overlapping ion series, making charge assignment

difficult.[18-20] By contrast, the MALDI ion source mostly generates singly, doubly charged peaks which could be easily assigned. Intact ions can be produced by laser irradiation on matrix crystal. When analyzing large ions, formation of particles is found in the size range from 10 nm to 1000 nm by irradiating MALDI matrix samples.[21, 22] The matrix particles will interfere with viral particles (the size range from 20 nm to 300 nm) during laser desorption process and thus hinder the analysis of large bioparticles. Moreover, when the particle mass becomes large (>100 kDa), its ion velocity is low, making high mass ion detection very challenging.[23-25] Besides, tandem mass analysis of MALDI ions is helpful to acquire the structure information, but it is not well studied yet for m/z > 12000.[26] The LIAD ion source is favorable in generating particles with the size greater than 50 nm by means of acoustic waves.[12, 27, 28] Multiple pre-charged ions can be generated without matrix interference and fitted to single particle analysis with both optical and charge detection.[12, 27] The drawback of LIAD ion source is low ion generation efficiency.

After ions are generated, they must be transported and guided to the mass analyzers for mass analysis. Typically, by reducing the guiding quadrupole driving frequency and increasing the buffer gas pressure, high mass ions can be cooled down and guided to mass analyzers.[29-33] Mass analyzers can be divided into ion trap and time-of-flight categories. Ion trap mass analyzers such as two dimensional[34-37] and

three dimensional quadrupole ion trap (QIT) [38, 39], DC gate ion trap[40] and orbitrap[31, 32, 41] show good trapping efficiency of large particles. Time-of-flight (TOF) mass analyzers can be run in linear, reflectron, and orthogonal modes and coupled with quadrupole for mass selection, ion activation and isolation.[29, 30] Moreover, no mass analyzers can fully cover the whole size ranges of nanoparticles. If the particle density is known, the particle size can be converted to particle mass. Therefore, differential mobility analysis (DMA) coupled with electrospray ion source offers an alternative approach to measure the effective particle sizes and thus characterize large biomolecules and nanoparticles ranging from a few nanometers to several hundred nanometers.[42-44]

Detectors are incorporated with mass analyzers to detect ions. The main reason that the conventional mass spectrometers cannot detect high mass ions is the use of a secondary electron detector, such as an electron multiplier and multi-channel plates (MCP) which cause low secondary electron yields of high mass ions. New detectors including a charge detector[27, 40], a nanomembrane detector[45, 46], a secondary ion detector[47, 48], an active pixel detector[49], and a cryodetector[50] are therefore designed and incorporated with mass analyzers to overcome that problem.[46, 47, 51, 52]

In general, when determining the masses of large biomolecules and bioparticles, we could divide mass spectrometric techniques into two categories. The first category

aims to measure the masses of intact particles including single particle quadrupole ion trap mass spectrometry[12, 28, 53], cell mass spectrometry[27, 54], charge detection mass spectrometry[40, 55, 56] and differential mobility mass analysis[42, 43]. In single quadrupole ion trap mass spectrometry and cell mass spectrometry, detectors such as light scattering, laser induced fluorescence, a charge detector and an electron multiplier are developed to overcome the detection limit of large biomolecules and bioparticles. Charge detection mass spectrometry adopts a non-destructive charge detector to sense the image charge of particles. Differential mobility mass analysis employs the condensation particle counters (CPCs) to optically detect nanoparticles. The second category focuses on the mass and tandem mass measurement of biomolecular ions including quadrupole ion trap mass spectrometry[57-59], time-of-flight mass spectrometry[23, 24, 46], quadrupole orthogonal time-of-flight mass spectrometry[29, 30] and orbitrap mass spectrometry[31, 32, 41]. Quadrupole ion trap mass spectrometry uses an electron multiplier to acquire mass spectra of large proteins. Time-of-flight mass spectrometry couples with several detectors including a microchannel plate detector, a secondary ion detector, a cryogenic detector, a nanomembrane detector, and a charge detector to extend the detection limit of large proteins. Quadrupole orthogonal time-of-flight mass spectrometry and orbitrap mass spectrometry can perform tandem mass analysis and high mass resolution analysis.

Quadruople orthogonal time-of-flight MS and orbitrap MS now play important roles in native mass spectrometry.[1] Large viral capsids, such as hepatitis B virus capsids and their fragmental ions are acquired with quadrupole orthogonal TOF MS.[19, 60] Orbitrap MS is now able to analyze large protein complexes up to 1 MDa and its tandem MS ability achieves MS^3 with high mass resolution.[31, 32] The high quality mass spectra enable high throughput study of large ESI ions. To streamline the identification of mass, stoichiometry and interactions of different subunits, new algorithms, such as AutoMass[19] and Massign,[20] are developed.

2. Ion Sources

2.1 Electrospray ionization

Dole *et al.* developed electrospray ionization to generate molecular beam of macroions.[61] Polystyrene macroions of molecular weight up to 411000 weight-average amu appear mostly to be multiply charged single species. An important milestone was hit by Fenn *et al.* who applied ESI technique to generate oligonucleotides and proteins and proteins with molecular weights up to 130000 Da were obtained.[7] Robinson *et al.* performed impressive mass measurement of bacteriophage MS2 viral capsid ions up to 2.5×10^6 Da and with a charge state of ~113.[62] Bacteriophage MS2 viral capsids remained intact during their flight and were

dissociated to monomeric subunits. Benner and Siuzdak *et al.* used ESI to generate tobacco mosaic viruses (TMV) in the gas phase with charges up to several hundred.[14] Hepatitis B virus (HBV)[60], norwalk virus[63] and bacteriophage HK97 viruses[64] with molecular weight of few MDa were generated by ESI and analyzed by modified Q-TOF instrument by Heck *et al.* The above studies demonstrated that ESI ion source coupled with mass spectrometry is a powerful analytical technique to generate macroions and obtain the structure information of ions.

2.2 Matrix-assisted laser desorption ionization

Tanaka *et al.* first generated polymer and proteins up to m/z 100000 with soft laser desorption/ionization of nanogold powder dispersed in glycerol and acquired the mass spectra.[8] Karas and Hillenkamp reported matrix-assisted laser desorption ionization by ultraviolet irradiation could obtain mass spectra of proteins.[9] Hillenkamp *et al.* further used infrared laser to acquire mass spectra of synthetic DNA, restriction enzyme fragments of plasmid DNA, and RNA transcripts up to a size of 2180 nucleotides.[25] Li *et al.* generated polymers up to 1.5 MDa and detected the doubly charged ion signals.[23] Not only polymers and proteins can be generated by MADLI ion source, but also nanomaterials can be formed in the gas phase, ZnS[65] and Pt[66] nanoparticles were detected with a TOF mass spectrometer. Low charge states of MALDI ions make the mass assignment simple and straight-forward.

2.3 Laser-induced acoustic desorption

Laser-induced acoustic desorption (LIAD) can generate large ions. Chen *et al.* adopted LIAD to desorb 20 μm size Al_2O_3 particles and cyctocrome C protein from sapphire substrate.[10] In addition, surface acoustic waves can detach particles from sample substrate surface and improves cleaning effectiveness as shown by Kolomenskii *et al.*[67] Viral particles, bacteria and cells are desorbed by LIAD with quadrupole ion trap mass spectrometry.[12, 27, 28]

3. Instrumentation

3.1 Quadrupole ion trap mass spectrometry and linear ion trap mass spectrometry

Quadrupole ion trap (QIT) is a suitable ion trap device for non-destructive mass measurement of single, trapped nanoparticles and for destructive mass measurement of large ions. The non-destructive mass measurement can be traced to 1950s.[68] Single microparticles were trapped and analyzed by light scattering, laser induced fluorescence, and charge detection methods. The destructive mass measurement is done with an electron multiplier and a charge detector. To eject ions, "mass selective instability" mode is applied in a quadrupole ion trap. Either rf amplitude or frequency must be scanned to acquire the mass spectra. Frequency-scan employs the wideband power amplifier, so it can easily cover wide mass range. Voltage-scan needs a power

amplifier to boost a transformer to several thousand volts. Due to high Q factor of a transformer, it is very difficult to cover wide mass range with voltage-scan. Therefore, frequency-scan is superior to voltage-scan.[54, 57, 69]

The advantage of linear ion trap (LIT) is its high ion capacity and MS^n ability.[34, 38] LIT is favorable to store more ions and allows tandem analysis of trapped ions. An electron multiplier and high buffer gas pressure would affect bioparticle detection with LIT.[70] High buffer gas is needed to cool down ions when the size of ions becomes larger, but an electron multiplier could not be operated in this condition. Typically conversion dynode voltage must be set high enough (> 10kV) to get high gain of ion signals, but high buffer gas pressure will cause discharging of an electron multiplier. A charge detector coupled with LIT-MS can work at high pressure condition without discharging problem and thus enhance the detection of high mass ion signals.

3.1.1 Electron multiplier

The sensitivity of a secondary electron detector (e.g. an electron multiplier and microchannel plates) decreases as $v^{4.4}$, where v is the velocity of the incident ion.[45, 46] This velocity relation leads to a remarkable decrease in sensitivity of those detectors for large and heavy ions. To detect high mass MALDI ions with an electron multiplier,

Schlunegger *et al*. firstly adopted three dimensional QIT with frequency-scan method to cover high mass range.[57] By using low frequencies (below 100 kHz) and low amplitudes (below 200 V), high mass singly charged bovine serum albumin (BSA) and immunoglobulin G (IgG) ions are trapped and analyzed by frequency sweep method. The instrument shows good sensitivity, signal-to-noise ratios (10:1), and a mass resolution of 70. Ding *et al*. proposed using a frequency-scan digital ion trap coupled with electrospray ionization (ESI) and atmospheric pressure matrix-assisted laser desorption/ionization (AP-MALDI) sources to demonstrate the capability of the digital method.[69] AP-MALDI mass spectra of singly charged horse heart myoglobin ions (17 000 Th) were generated using a trapping voltage of only 1000 V and a mass resolution of 2100 is reached. Recently, McLuckey *et al*. developed mass-selective instability analysis by scanning a direct current (dc) voltage applied to the end-cap electrodes while holding the radio frequency (rf) potential at a fixed value in a QIT.[59] They ejected ions along the $ß_z = 0$ instability line in the direction from high mass-to-charge (m/z) to low m/z. Doubly charged pyruvate kinase ions were observed at m/z ~ 131 000. The combination of QIT and an electron multiplier detector suffers from poor ion-secondary electron conversion efficiency and low ion ejection velocity and therefore the ion detection efficiency of high mass ions is poor.

Commercial LIT MS operated in the frequency of ~1 MHz can detect mass

range up to m/z ~4,000. In order to extend mass range of LIT MS, Chen *et al*. developed a home-made frequency-scan LIT mass spectrometer with low rf driving frequency. They adopted frequency-scan method to cover the wide mass range and raised the conversion dynode voltage up to -30 kV to increase secondary electron signals. Singly charged secretory immunoglobulin A (385 kDa) ions were detected. Reilly *et al*. demonstrated singly-charged, intact proteins in the range of 10 to 200 kDa and 1.5 MDa urea particles can be detected by a linear quadrupole ion trap.

3.1.2 Light scattering

Photon is a fundamental light particle and used by light scattering method to detect ions because of its high sensitivity. Millikan's oil drop experiment is the first one to measure charges of microparticles by light scattering method.[71] Wuerker *et al*. demonstrated the capability of trapping and detection of single microparticles using a QIT mass spectrometer.[68] Hars and Tass further proposed measuring the star-like ion motion in the radial plane to determine the mass of a single particle in the range of 10^{9}-10^{12} Da with accuracy of 10^{-3};[72] however, changes in charge states are not obvious because of multi-particle clumping during the injection of ions. Schlemmer *et al*. developed fast Fourier transform technique to measure the single particle mass at r-z plane.[73, 74] 500 nm SiO_2 particles were trapped in an ion trap with resolution (mass deviation) of 10^{-4} in a 10 s measurement. Cai *et al*. further used QIT to trap and eject

microparticles, and ions were detected via light scattering method.[75, 76] Single particle mass spectra were acquired in mass-selective instability mode. But absolute charge states of trapped particles were not known in this study. Peng *et al*. observed a stationary star pattern by fine-tuning driving frequency to resonate with the radial secular frequency in a QIT and obtained an analytical formula of secular frequency that is valid for $q_z<0.8$.[12, 53] Intact single *Escherichia coli* cells were generated by MALDI ion source and their absolute mass was measured.[53] Besides, with laser induced acoustic desorption (LIAD) ion source, viruses, bacteria, and mammalian whole cells can be generated without confusion caused by MALDI clusters. The m/z of a particle can be measured with very high precision up to 10^{-4}.[77, 78] The QIT MS adopted an averaging peak-to-peak voltage detector to measure rf amplitude which is traced to a standard rf source and therefore QIT MS can be used as particle mass standard measurement with the particle size greater than 300 nm.[78]

Trevitt *et al*. combined the secular frequency measurement with Mie scattering measurement of single particle and found small uncertainties in secular frequency measurement resulted in significant errors in the absolute mass and charges. But the misalignment of QIT electrodes is small and trap parameter z_0 is appropriate.[79] To overcome low light collecting efficiency of QIT, Nie *et al*. used a cylindrical ion trap (CIT) to replace the end-cap electrodes by an electrically conductive glass plate that

enables collection >10% of light radiating from the trapped particle. They successfully detected recombinant human adenovirus type 5 (Ad5), grouper iridovirus (GIV), and vaccinia virus (VV) with sizes range from 80 to 300 nm.[28]

3.1.3 Laser induced fluorescence

Laser induced fluorescence (LIF) is widely used in flow cytometry to measure the size distribution of nanoparticles. Cai *et al*. firstly attempted to integrate the LIF with QIT to confine single particles with mass larger than 5 MDa in a trap.[80] They successfully observed individual fluorescent 27 nm nanospheres which contains 180 fluorescein dye equivalents and an average signal-to-noise ratio of 10 has been achieved. Moreover, they adopted another QIT to cool nanoparticles inside the QIT and monitor LIF of trapped particles to acquire the mass spectra of single particles.[58, 80] This configuration extended the mass analysis of nanoparticles with $m/z > 10^5$.[5] Recently, Talbot *et al*. used LIF to visualize populations of gaseous ions stored in a quadrupole ion trap (QIT) mass spectrometer. This technique might help understand the collective ion motion and the ejection behavior of high mass ions under high buffer gas pressure.[81]

3.1.4 Charge detector

Single particle QIT mass spectrometry can measure intact bioparticles, including viruses, bacteria, and whole mammalian cells with high precision.[4] But it takes about 15–30 minutes to determine the absolute mass of each trapped particle. Peng *et al*. first proposed charge-monitoring laser-induced acoustic desorption mass spectrometry (CMS) for rapid mass measurement of cells and microparticles.[27, 54] The CMS simultaneously measure both the mass-to charge ratio (m/z) and total charges (z) of a particle. Typically more than 5 particles with S/N ratio of 10 are acquired in one second. The background noise of the charge detector is about 500 e. CMS successfully measured different types of mononuclear cells ($CD3^+$ lymphocytes and $CD14^+$ monocytes) and cancer cells. Nie *et al*. followed this approach to acquire mass and mass distributions of different red blood cells.[82] Mass resolution of ~100 and mass accuracy of ~1% can be achieved with this frequency-scan CMS.[83] Chen *et al.* measured the mass distribution of sinapinic acid matrix clusters from monomer to MDa region with a CMS.[22] In CMS, harmonic interference noises from an AC power source and rf voltage interference noise from rf field affect the detection of a charge detector. Chou *et al.* proposed an orthogonal wavelet packet decomposition (OWPD) filtering approach to denoise interference from the acquired mass spectra. Mass spectra of microparticles and *Escherichia coli* are obtained without rf interference.[84] When rf is applied on a QIT in high pressure condition (~80 mTorr), undesired arcing

is produced; therefore, Xiong *et al.* adopted rectangular and triangular waveforms to reduce the onset voltage and found their mass resolution is the same as that of conventional sinusoidal waveform.[85] Moreover, rectangular waveform technique can detect large ions with a digital ion trap,[69] which fosters the development of miniature instrument with switching circuits instead of power amplifier. The power of CMS instrument can be greatly reduced. To reduce the size of ion trap, Nie *et al.* have shown that a miniature cylindrical ion trap mass spectrometer (CIT-MS) equipped with a mechanical pump can measure the masses of cells and microparticles.[86]

In applications, CMS is used to measure the quantity of nano-/microparticles as efficient carriers for drug delivery.[87, 88] Quantitative measurement of the cellular uptake of nano-/microparticles is of great importance for the elucidation of the mechanisms of cell endocytosis and exocytosis. We found CMS coulb be used to measure not only the cellular uptake of metal nanoparticles but also that of nonmetal nano-/microparticles and greatly reduced analysis time as compared to conventional approaches such as inductively coupled plasma mass spectrometry (ICP-MS) which limits to metal nanoparticles. Nie *et al.* used CMS to characterize the column packing materials in high-performance liquid chromatography (HPLC).[89] The mass deviation of the silica particles after modification by different length of alkyl chains can also be determined using CMS. The specific surface area, carbon load, and size distribution

of packing materials are characterized simultaneously too. Nie *et al.* showed CMS can be incorporated with an ambient desorption source to measure masses of microparticles.[90] The ambient desorption method exploited the discontinuous atmospheric pressure interface (DAPI) to generate and desorb microparticles under atmospheric pressure with a pulsed airflow as shown in Figure 1. Bacteria, cells, polystyrenes, synthetic diamonds, and silica particles can be directly desorbed in ambient condition.

Furthermore, a charge detector can measure the quantity of molecules. Peng *et al.* first measured the C_{60} signals with a QIT MS.[27] Chen *et al.* measured IgG and IgM ions.[91] To increase the number of ions and ion signal, a possible way is to incorporate a charge detector with LIT-MS.

3.2 Time-of-flight mass spectrometry

MALDI ion source is frequently coupled with time-of-flight (TOF) mass spectrometer.[92] The mass range of TOF MS should be unlimited in theory; however, its mass range is limited by the sensitivity of a detector in practice. Conventional secondary electron detectors, e.g. MCP are incorporated with TOF MS and the detection limit is < 1 MDa. Secondary ion detectors, cryogenic detectors, and nanomembrane detectors are proposed to overcome the detection limit of TOF MS

and now are able to detect ions with mass > 1 MDa.

3.2.1 Microchannel plates

The microchannel plate detector is widely used in TOF MS. Detection of human IgM at m/z approximately 1 MDa is achieved by Williams *et al*.[24] Li *et al.* further demonstrated the detection of doubly charged polystyrene signals with molecular weight up to 1.5 million.[23] But the signal-to-noise ratio is poor and close to upper limit of a MCP detector. To enhance the sensitivity of a MCP detector, Heeren *et al.* developed an active pixel detector (MCP-based detection system). The S/N ratio can be improved to a factor of ~4 in detecting IgA molecules.[49]

3.2.2 Secondary ion detector

A Daly detector is a gas ion detector which consists of a metal doorknob, a scintillator (phosphor screen) and a photomultiplier.[93] It was widely used in mass spectrometers. Zenobi *et al.* collected the photons produced by the impact of ion packets with a scintillator and demonstrated that an ion-to-photon detector showed about 10 times higher signals than the MCP for heavy ions (150 kDa).[48] Wang *et al.* further developed a bipolar ion detector (BID) to detect secondary ions rather than secondary electrons with a conversion dynode voltage at -25 kV. For ions with m/z ~

90 000, the sensitivity of the BID is 1.4-14.4 times that of the MCP.[47]

3.2.3 Cryogenic detector

Phonons are elementary excitations of crystal lattice. When ions impinge the cryogenic detector, heats are generated and transferred to collective vibrations on normalinsulator-superconductor (NIS) microcalorimeter device near absolute zero temperature.[94] A very small change in temperature resulting from interaction of NIS microcalorimeter device and a particle leads to a significant change in resistance. The junction current is measured by a high-speed low-noise series-array superconducting quantum interference device (SQUID) preamplifier. Measuring the phonons is therefore dependent on the energy not on particle masses and velocity of ions. Frank *et al.* introduced a low-temperature calorimetric detector to measure kinetic energy of individual incident ions irrespective of their masses or charge state.[95, 96] Cryogenic microcalorimeters and superconducting tunnel junctions are velocity independent and phonon of ions at temperatures lower than hundred millikelvin are measured. Recently, Zenobi *et al.* showed a 16-element superconducting tunnel junction (STJ) detector coupled with a fully adjustable gimbal-mounted ion source/focusing region can allow unparalleled sensitivity for detection of singly charged immunoglobulin M ions (~1MDa).[97] Bier *et al*. further used the same 16 STJs detector and detected

polystyrene ions and virus capsids up to 2 MDa and 13 MDa, respectively.[98, 99] These cryogenic particle detectors show good mass sensitivity at high mass range, but the drawbacks of cryogenic detectors are expensive cryogenic cooling unit, low active detection areas and long response time, and thus restrict their practical use.

3.2.4 Nanomembrane detector

A nanomembrane detector based on mechanical deformation and vibration of a nanomembrane is developed to overcome the detection of high mass ions by Blick *et al.*[45, 46] Figure 2 shows the schematic design of nanomembrane detector with TOF MS. Mechanical vibrations of the nanomembrane excited by ion bombardment translate into corresponding oscillations in the field emission current. The modulated field emission current is amplified by the microchannel plate (MCP). High mass proteins such as IgG and IgM are measured with high mass resolution of 129±44 and 250±48. In the right inset of Figure 2,[45] the mass resolution (m/Δm) becomes better as molecular mass is increasing, which is because the rise time and decay constant are highly independent on both mass and kinetic energy of the ion, and the time resolution is highly dependent on the effective cooling of the silicon nanomembrane via field emission.

3.2.5 Charge detector

Hillenkamp *et al.* developed a charge detector for ion detection in MALDI-TOF instruments. The charge detector comprises a 18 mm-diameter metal electrode as a Faraday charge collector and a charge-sensitive FET preamplifier. A net charge of 1.8×10^4 is required for S/N ratio of 2. IgG ions can be detected with S/N ratio > 10. With rise time of 25 ns, mass resolution for MALDI ion detection is not restricted to a charge detector. To increase the sensitivity of a charge detector, Bouyjou *et al.* developed a16-channel low power CMOS device and reached an equivalent noise charge of 318 e^-.[100]

3.3 Charge detection mass spectrometry

Charge detection mass spectrometry (CDMS) measures the image charge of ions. Image charge detection of microparticles was first reported in 1960 by Shelton *et al*., who used pairs of conducting metal plates inside a shielded cylinder to detect charged iron spheres in a high voltage accelerator system.[101] With known time-of-flight of ions, absolute masses of ions thus can be calculated. To measure the absolute masses of particles accurately, two types of measurement were developed to increase the signal-to-noise ratio. First is the recirculating trap which allows multiple paths of ions in an electrostatic DC ion trap.[40] Second is the linear array which can extend the

detection limit by $\sqrt{2}$ with multiple sensing stages.[56]

3.3.1 Recirculating trap

Benner designed a gated electrostatic ion trap that can repetitiously measure the charge and m/z of large electrospray ions.[40] The schematic design of this instrument is shown in Figure 3. Once a single ion passing through the detector tube, the detector displays an amplifier noise of 50 electrons. After averaging, noise can be reduced to 5 electrons. Jarrold *et al*. showed cooling of the JFET can increase its transconductance and lower thermal noise, and thus improve the signal to noise (S/N) ratio.[55] Single ions with 9 elementary charges have been detected while ADH monomer ions with 32 to 43 charges were trapped over 1500 cycles and the measured image charge is around 2.2 electrons. With CDMS, Jarrold *et al.* further measured the mass (23.6 MDa) and charge (427e) of bacteriophage P22 procapsids[102] and detected intermediates of hepatitis B virus capsids[103].

3.3.2 Linear array

Another thought to reduce noise is to arrange charge detectors in series. In Figure 4, Gamero-Castano *et al*. showed the design and carefully calculated its charge detection limit.[56] The detection limit and standard error of the charge measurement can be reduced by factors of $\sqrt{2}$ and $\sqrt{n}$. Measurement of a droplet with time of

flight of 493 μs and charge noise of ~100 electrons were demonstrated.

3.4 Differential mobility analysis

Differential mobility analysis (DMA) is a routine analysis method used to rapidly characterize viruses and virus-like particles.[42, 44] A DMA device is composed of four major elements: a gas flow, a neutralizer, an electric field which is generated by two flat electrodes and perpendicular to the gas flow, and a condensation particle counter (CPC) placed at the end of one electrode for particle detection as depicted in Figure 5.[43] In a DMA device, a charged particle is driven by two forces, drag force (related to gas flow, particle drift, and particle size) and electric force (generated by the interaction between electric field and particle charge). Specific particles can drift into CPC in exact conditions; therefore, DMA is capable of separating charged particle based on their m/z or gas-phase electrical mobility.[42] Unlike typical MS analyzers, drag force provides a big effect on particle motion because DMA is operated at near atmospheric pressure with gas flow. So, the information of particle sizes can be offered by DMA analysis.

Charge reduced electrospray differential mobility analysis (ES-DMA) can quantitatively analyze particle sizes from 0.7 to 800 nm. The notable precision of 24 nm particles separated by ES-DMA is 1.2 nm (standard derivation).[104] The ES-DMA

is suitable for size analysis of whole viruses and virus fragments. For instance, S. Guha *et al*. measured the PR772 and PR7 with ES-DMA, and the mean sizes were determined to be 62.1 ± 0.4 nm and 23.0 ± 0.3 nm, respectively.[105] Hogan *et al*. also analyzed bacteriophage MS2 and found its diameter was 24.13 ± 0.06 nm while the capsid heads of large bacteriophages T2 and T4 88.32 nm ± 1.02 nm and 87.03 ± 0.18 nm, respectively.[43] Besides, ES-DMA has capability of measuring the concentration of virus in solution. Cole *et al*. determined the particle concentration of three bacteriophages MS2, PP7, and □X174 which were similar to amino acid analysis in most cases.[106]

3.5 Quadrupole orthogonal time-of-flight mass spectrometry

Using nanoflow electrospray with time-of-flight mass analysis, Robinson *et al*. showed that it is possible to obtain definitive charge states in the spectra of large multiprotein complexes.[107] In Figure 6a, GroEL complex shows a series of peaks centered at *m*/*z* 10000. Next, bacteriophage MS2 was proved to maintain the intact capsid in vacuum and had undergone collision-induced dissociation (CID) with neutral gas molecules and the CID mass spectrum was shown in Figure 6b.[62] Heck *et al*. further modified the Q-TOF 1 instrument including the introduction of enhanced pressure and altered electronics (e.g. quadrupole frequency, collision energy and TOF

pusher frequency), as well as specialized detectors to improve transmission and measurement of very large ions.[30] The instrument design is shown in Figure 7. HBV capsids of 90 and of 120 dimers with masses of 3 and of 4 MDa were determined from m/z 20000 to 30000.[60, 108] The measured precision of both capsids is within 0.1%. 10.1 MDa norwalk virus-like particles were measured as a function of solution pH, ionic strength, and capsid protein concentration.[63] Figure 8 shows the intact 18 MDa capsids of bacteriophage HK97 measured with modified Q-TOF 1 instrument with a charge number of 350.[64] It is noted that incomplete desolvation of specimen causes the peak separation and overlapping around 40 GDa which limits the detection of large protein complexes from GDa to MDa.

3.6 Orbitrap mass spectrometry

With an orbitrap mass analyzer, intact protein assemblies with molecular weight approaching one million Daltons were measured by Cooks[41] and Heck *et al.*[31, 109] Since the introduction of the first orbitrap-based mass spectrometer in 2006, this mass analyzer has become increasingly popular.[110-112] The orbitrap mass spectrometers are used to analyze small molecules and peptides, but now these instruments can be modified to analyze very large native protein assemblies. Shown in Figure 9 is a dedicated instrumental modifications of an Exactive Plus instrument (ThermoFisher

Scientific) with a higher-energy collision-induced dissociation (HCD) option. Briefly, the modifications include altering software to allow detection of ions at higher *m/z* range, tuning radiofrequency voltages of transport multipoles and altering the pressure in the HCD cell. CsI clusters up to *m/z* of 18,000 were detected and a resolution of 25,000 was achieved at *m/z* of 5,000 and a resolution of 16,000 was obtained at *m/z* of 10,000. The full width at half maximum (FWHM) resolution of GroEL peaks (68+ to 77+ at *m/z* of 10,000 to 12,000) was close to 4,000, and the experimental molecular weight was close to 1 MDa. Moreover, glycoforms for an antibody-based construct with a very heterogeneous glycan pattern were resolved and assigned.[109] A few femtomoles of samples were required and data acquisition of single mass spectrum was in few seconds. A resolution up to 12000 at m/z 6000 could be achieved with high mass accuracy (~0.001%), thus allowing the assignment of modified antibodies. Kelleher and Makarov *et al.* further modified the Q Exactive plus instrument with orthogonal ion injection interface, two ion funnels, a quadrupole filter and a high pressure HCD cell (10^{-2} mbar).[32] The signal-to-noise ratio can be enhanced with orthogonal ion injection and ion funnels and the injection time was greatly reduced. The ion transmission was extended to m/z 20000 and ions can be mass-selected in this mass range. Isolation window was about 70 in the m/z range exceeding 10000 Th. Tandem MS analysis of large protein complexes, such as phosporylase B (194 kDa),

pyruvate kinase (232 kDa), and GroEL (801 kDa) can be reached to MS^3.

4. Algorithms

Electrospray ionization coupled to native mass spectrometry (MS) has evolved as an important tool in structural biology to decipher the composition of protein complexes.[1, 20, 113] Commercial MS software was successfully developed to investigate and assign mass spectra of proteins or peptides. It is proper for the identification of charge state series of protein complexes as the charge state series are sufficiently separated. However, overlapping charge state distributions, fine structure and peak broadening of heterogeneous samples hamper mass analysis. To facilitate mass analysis, theory development and automation in the pre-processing of raw mass spectra, assigning peaks to ion series and deciphering the subunit compositions are discussed as below.

4.1 Theory

Conventional approach to assign ESI mass spectra of proteins was first invented by Mann *et al*. They developed the first averaging and deconvolution algorithm to assign charge states in ESI mass spectra of protein complexes.[114] The "averaging algorithm", assigns charge numbers to the ions associated with the m/z value for each

peak and averages the resulting masses to give a best estimate of the molecular masses. The "deconvolution algorithm", transforms several peaks of multiply charged ion into one peak corresponding to a singly charged ion as shown in Figure 10. Moreover, maximum entropy approaches are often used to find the best assignment and reduce the complexity in the spectra based on deconvolution algorithm.[115-120] These approaches are useful to analyze proteins of intermediate masses, but are not able to correctly assign charge states of larger protein complexes, e.g. viral capsids or nano-/microparticles. Peng *et al*. introduced an LeastMass algorithm which is able to achieve the charge states assignment of very high mass ions created by ESI.[18] This algorithm searches a series of m/z peaks which can match the charge ratio as input and the molecular mass are obtained by taking into account all possible charge states. The plot of S/<m> vs. z or <m>, where S is the standard deviation, z is the ion charge, and <m> is the mean mass, shows a periodic pattern when the correct charge assignment is identified. The periodic pattern could be explained with the minimum standard deviation theory, in which a harmonic oscillation indicates a correct charge state assignment. Shown in Figure 11 is the analysis of HBV capsids. The periodic pattern is observed in *T=3* and *T=4* ions when the correct charge is matched. However, a selection of mixture peaks of *T=3* and *T=4* ions results in the loss of periodicity. LeastMass can also help assign the correct charge states of single plasmid

DNA and PEG ions analyzed by Fourier transform ion cyclotron resonance (FTICR) mass spectrometer[121, 122] and 18 MDa capsids of bacteriophage HK97 by QTOF 1 instrument [64].

4.2 Raw data processing

Raw data processing is of importance to reduce analysis time. An algorithm that can handle noisy raw mass spectra is necessary. The data pre-processing requires thorough smoothing, background subtraction, and an automatic threshold determination. This is especially challenging when the signals are highly deformed and mixed with noises.[19] The automatic pre-processing software can greatly reduce analysis time and keep fidelity of acquired mass spectra.

4.3 Search engine

A search engine, AutoMass, was developed by Peng *et al*. to automatically assign ion series to peaks by game theory.[19] AutoMass can define the correct boundary between different distributions to yield accurate masses. It helps analyze the masses and the boundary of heterogeneous protein assemblies with overlapping charge state distributions, fine structure, and peak broadening. The boundaries of ion series in the well-resolved tandem mass spectra of the hepatitis B virus (HBV) capsids and those

of the mass spectrum from CRISPR-related cascade protein complex are accurately assigned. In Figure 12, complicated tandem mass spectra derived from intact HBV capsids at high collision energy conditions are analyzed. The generated HBV tandem mass spectra of *T = 3* and of *T = 4* precursor ions with an accelerating voltage of 400 V are depicted in Figure 12a,c, and tandem mass analysis by AutoMass are shown in Figure 12b,d, respectively. The deviation of the predicted and the measured oligomer masses is less than 0.03%, far less than a single protein subunit. Moreover, less well-resolved mass spectra, for example, the norovirus capsid mass spectra at different levels of desolvation are analyzed as well.

4.4 Subunit complexes assignment

Morgner *et al*. introduced Massign to optimize data analysis by reducing spectra size, smoothing and subtracting background, identifying peaks, assigning ion series and the number of possible subunit combinations by integrating information from multiple sources.[20] By adding connectivity and stoichiometry restraints into the software, Massign reduces the number of potential complexes to one or two as shown in Figure 13. In practice, the ion boundary has to be manually refined and potential mass range, m/z range, and maximum possible charge are needed to be inputted manually. Benesch *et al*. developed CHAMP software which can estimate the

distribution of different stoichiometries from overlapping and unresolved peaks.[123] It is similar to SOMMS[120] but is more user-friendly. Thalassinos *et al*. developed the Amphitrite software,[124] which is favorable to analyze ion mobility data and is comparable to CHAMP and SOMMS in peak assignment. It can retrieve or compare different ion shapes from very complex samples.

5. Choice of mass spectrometer

The mass spectrometric techniques are summarized in table 1. In the following, we will discuss how to choose a proper mass spectrometric technique. Firstly, to measure masses of microparticles (e.g. cells), a quadrupole ion trap with a charge detector would be favorable because it can measure masses and mass distribution of cells in a short period of time.[27] Besides, it can measure mass difference before and after cellular uptake of nanoparticles and adhesion of moleclues on microparticle surfaces and columns.[87, 89] Secondly, a quadrupole ion trap with light scattering can measure masses of single virus, bacteria and cells with high precision.[12, 53] With this technique, changes in mass due to adhesion of molecules on single nano-/microparticles in vacuum can be studied. Thirdly, charge detection mass spectrometry can measure the masses of viruses;[14, 103] however, multiple charge nature of ESI causes wide mass distribution of ions and limits its application. Fourthly, ESI

differential mobility analysis (DMA) is an alternative instrument to acquire the size distribution of nanoparticles rapidly.[43] Fifthly, orbitrap[31, 41] and orthogonal quadrupole time-of-flight mass analyzers[62, 64] allow mass analysis of intact virus capsids and large proteins. Tandem mass analysis offers the structure information.[31] But when particle size becomes larger, higher energy is required to activate and dissociate those bioparticles**.** During activation and dissociation of nanoparticles, trapping frequency in an ion trap device is not able to cover a board range. Tandem in space is therefore favored than tandem in time technique.[125, 126] Mann *et al.* showed that dual linear ion trap orbitrap instrument can increase sequence speed in proteomics research.[127] Dual ion traps provide a possible solution to dissociate large ions to fragments by combining both tandem in time and tandem in space techniques.[58, 128] Sixthly, with the help of AutoMass and Massign programs, analysis time of complicated ESI mass spectra can be greatly reduced. However, automated data preprocessing is required to minimize the effect of deformed mass spectra of heterogeneous protein complexes, reduce the size of data and speed up the analysis time. Seventhly, pulse nature of MALDI ion source is suitable to couple with time-of-flight mass analyzer to acquire simple mass spectra. TOF-MS with a cryogenic detector, an active pixel detector and a nanomembrane detector can now extend mass detection from hundred kDa to MDa. But tandem mass analysis of high mass ions in a TOF-TOF instrument and low

ionization efficiency of MALDI ion source in detecting large bioparticles (>100 kDa) are still very challenging. The use of a charge detector with TOF MS and quadrupole ion trap MS can help understand quantity of ions and examine the possible ionization mechanism. Finally, mass resolution in high mass range and isotopic analysis of high mass biomolecules[129] are still challenging for both FTICR and orbitrap mass analyzers.

6. Conclusions and Future Outlook

Single particle quadrupole mass spectrometry approach provides accurate mass measurement with particle sizes from 80 nm to 10 μm.[4] But it is not suitable for high speed analysis. Cell mass spectrometry offers destructive measurement of cells with sizes from 700 nm to 30μm.[27] It offers high speed analysis of cells. Charge detection mass spectrometry proposed non-destructive determination of particle charges. The signal-to-noise can be enhanced with increasing multiple paths of ions. The use of a cryogenic detector in TOF MS can extend the detection limit up to 2 MDa.[98] With nanomembrane detectors, IgM molecules can be detected with TOF MS with a resolution of ~250.[45] Differential mobility analysis (DMA) is now available to rapidly characterize viruses and virus-like particles. 18 MDa viral particles with charges up to 350 are explored.[64] The mass resolution has reached the instrumental limit of

quadrupole orthogonal TOF MS. Orbitrap MS might be a promising solution to improve mass resolution in analyzing large bioparticles to MDa mass range.[32] The AutoMass, a game theory based search engine, can successfully assign the very complicated tandem mass spectra of HBV capsids with m/z from 40000 to 80000.[19] Moreover, Massign can simplify the assignment of different subunit combinations in large heterogeneous systems.[20] Overall, mass spectrometric techniques are powerful tools and continuing to provide valuable mass and structure information of large biomolecules and bioparticles.

DISCLOSURE STATEMENT

The author is not aware of any affiliations, memberships, funding, or financial holdings that might be perceived as affecting the objectivity of this review.

ACKNOWLEDGMENTS

The author thanks National Dong Hwa University (NSC 102-2112-M-259-003-MY3) and the National Science Council of Taiwan, Republic of China, for continuous support of his work over the past six years.

LITERATURE CITED

1. A. J. R. Heck, *Nat Methods*, 2008, **5**, 927-933.
2. E. D. Levy, E. B. Erba, C. V. Robinson and S. A. Teichmann, *Nature*, 2008, **453**, 1262-U1266.
3. C. S. Kaddis and J. A. Loo, *Anal. Chem.*, 2007, **79**, 1778-1784.
4. H.-C. Chang, *Annual Review of Analytical Chemistry*, 2009, **2**, 169-185.
5. W.-P. Peng, Y. Cai and H.-C. Chang, *Mass Spectrometry Reviews*, 2004, **23**, 443-465.
6. G. L. Glish and R. W. Vachet, *Nat Rev Drug Discov*, 2003, **2**, 140-150.
7. J. Fenn, M. Mann, C. Meng, S. Wong and C. Whitehouse, *Science*, 1989, **246**, 64-71.
8. K. Tanaka, H. Waki, Y. Ido, S. Akita, Y. Yoshida, T. Yoshida and T. Matsuo, *Rapid Communications in Mass Spectrometry*, 1988, **2**, 151-153.
9. M. Karas and F. Hillenkamp, *Anal. Chem.*, 1988, **60**, 2299-2301.
10. V. V. Golovlev, S. L. Allman, W. R. Garrett, N. I. Taranenko and C. H. Chen, *International Journal of Mass Spectrometry and Ion Processes*, 1997, **169–170**, 69-78.
11. J. L. Campbell, K. E. Crawford and H. I. Kenttämaa, *Anal. Chem.*, 2004, **76**, 959-963.
12. W. P. Peng, Y. C. Yang, M. W. Kang, Y. K. Tzeng, Z. X. Nie, H. C. Chang, W. Chang and C. H. Chen, *Angew Chem Int Edit*, 2006, **45**, 1423-1426.
13. Z. Ouyang, Z. Takáts, T. A. Blake, B. Gologan, A. J. Guymon, J. M. Wiseman, J. C. Oliver, V. J. Davisson and R. G. Cooks, *Science*, 2003, **301**, 1351-1354.
14. S. D. Fuerstenau, W. H. Benner, J. J. Thomas, C. Brugidou, B. Bothner and G. Siuzdak, *Angew Chem Int Edit*, 2001, **40**, 542-544.
15. J. L. P. Benesch, B. T. Ruotolo, D. A. Simmons, N. P. Barrera, N. Morgner, L. Wang, H. R. Saibil and C. V. Robinson, *Journal of Structural Biology*, 2010, **172**, 161-168.
16. P. Wang and J. Laskin, *Angewandte Chemie International Edition*, 2008, **47**, 6678-6680.
17. G. Siuzdak, B. Bothner, M. Yeager, C. Brugidou, C. M. Fauquet, K. Hoey and C.-M. Change, *Chem Biol*, 1996, **3**, 45-48.
18. Y. H. Tseng, C. Uetrecht, A. J. R. Heck and W. P. Peng, *Anal. Chem.*, 2011, **83**, 1960-1968.
19. Y.-H. Tseng, C. Uetrecht, S.-C. Yang, A. Barendregt, A. J. R. Heck and W.-P. Peng, *Anal. Chem.*, 2013, **85**, 11275-11283.
20. N. Morgner and C. V. Robinson, *Anal. Chem.*, 2012, **84**, 2939-2948.

21. S. Alves, M. Kalberer and R. Zenobi, *Rapid Communications in Mass Spectrometry*, 2003, **17**, 2034-2038.
22. S.-H. Lai, K.-H. Chang, J.-L. Lin, C.-L. Wu and C.-H. Chen, *Chemical Physics Letters*, 2013, **561–562**, 142-146.
23. D. C. Schriemer and L. Li, *Anal. Chem.*, 1996, **68**, 2721-2725.
24. R. W. Nelson, D. Dogruel, P. Williams and R. Beavis, *Rapid Communications in Mass Spectrometry*, 1994, **8**, 627-631.
25. S. Berkenkamp, F. Kirpekar and F. Hillenkamp, *Science*, 1998, **281**, 260-262.
26. Z. Liu and K. L. Schey, *Journal of the American Society for Mass Spectrometry*, 2005, **16**, 482-490.
27. W. P. Peng, H. C. Lin, H. H. Lin, M. Chu, A. L. Yu, H. C. Chang and C. H. Chen, *Angew Chem Int Edit*, 2007, **46**, 3865-3869.
28. Z. X. Nie, Y. K. Tzeng, H. C. Chang, C. C. Chiu, C. Y. Chang, C. M. Chang and M. H. Tao, *Angew Chem Int Edit*, 2006, **45**, 8131-8134.
29. F. Sobott, H. Hernandez, M. G. McCammon, M. A. Tito and C. V. Robinson, *Anal. Chem.*, 2002, **74**, 1402-1407.
30. R. H. H. van den Heuvel, E. van Duijn, H. Mazon, S. A. Synowsky, K. Lorenzen, C. Versluis, S. J. J. Brouns, D. Langridge, J. van der Oost, J. Hoyes and A. J. R. Heck, *Anal. Chem.*, 2006, **78**, 7473-7483.
31. R. J. Rose, E. Damoc, E. Denisov, A. Makarov and A. J. R. Heck, *Nat Meth*, 2012, **9**, 1084-1086.
32. M. E. Belov, E. Damoc, E. Denisov, P. D. Compton, S. Horning, A. A. Makarov and N. L. Kelleher, *Anal. Chem.*, 2013, **85**, 11163-11173.
33. I. V. Chernushevich and B. A. Thomson, *Anal. Chem.*, 2004, **76**, 1754-1760.
34. D. J. Douglas, A. J. Frank and D. Mao, *Mass Spectrometry Reviews*, 2005, **24**, 1-29.
35. J. W. Hager, *Rapid Communications in Mass Spectrometry*, 2002, **16**, 512-526.
36. J. C. Schwartz, M. W. Senko and J. E. P. Syka, *Journal of the American Society for Mass Spectrometry*, 2002, **13**, 659-669.
37. Z. Ouyang, G. Wu, Y. Song, H. Li, W. R. Plass and R. G. Cooks, *Anal. Chem.*, 2004, **76**, 4595-4605.
38. R. E. March and J. F. J. Todd, *Quadrupole ion trap mass spectrometry*, Wiley-Interscience, 2005.
39. R. E. March, *J Mass Spectrom*, 1997, **32**, 351-369.
40. W. H. Benner, *Anal. Chem.*, 1997, **69**, 4162-4168.
41. Q. Hu, R. J. Noll, H. Li, A. Makarov, M. Hardman and R. Graham Cooks, *J Mass Spectrom*, 2005, **40**, 430-443.
42. L. F. Pease Iii, *Trends in Biotechnology*, 2012, **30**, 216-224.

43. C. J. Hogan, E. M. Kettleson, B. Ramaswami, D.-R. Chen and P. Biswas, *Anal. Chem.*, 2006, **78**, 844-852.
44. S. Guha, M. Li, M. J. Tarlov and M. R. Zachariah, *Trends in Biotechnology*, 2012, **30**, 291-300.
45. J. Park, Z. Aksamija, H.-C. Shin, H. Kim and R. H. Blick, *Nano Letters*, 2013, **13**, 2698-2703.
46. J. Park, H. Qin, M. Scalf, R. T. Hilger, M. S. Westphall, L. M. Smith and R. H. Blick, *Nano Letters*, 2011, **11**, 3681-3684.
47. M.-H. Li, S.-T. Tsai, C.-H. Chen, C. W. Chen, Y. T. Lee and Y.-S. Wang, *Anal. Chem.*, 2007, **79**, 1277-1282.
48. F. Dubois, R. Knochenmuss and R. Zenobi, *Rapid Communications in Mass Spectrometry*, 1999, **13**, 1958-1967.
49. S. R. Ellis, J. H. Jungmann, D. F. Smith, J. Soltwisch and R. M. A. Heeren, *Angewandte Chemie International Edition*, 2013, **52**, 11261-11264.
50. W. H. Benner, D. M. Horn, J. M. Jaklevic, M. Frank, C. Mears, S. Labov and A. T. Barfknecht, *Journal of the American Society for Mass Spectrometry*, 1997, **8**, 1094-1102.
51. I. S. Gilmore and M. P. Seah, *International Journal of Mass Spectrometry*, 2000, **202**, 217-229.
52. G. Westmacott, M. Frank, S. E. Labov and W. H. Benner, *Rapid Communications in Mass Spectrometry*, 2000, **14**, 1854-1861.
53. W.-P. Peng, Y.-C. Yang, M.-W. Kang, Y. T. Lee and H.-C. Chang, *Journal of the American Chemical Society*, 2004, **126**, 11766-11767.
54. W. P. Peng, H. C. Lin, M. L. Chu, H. C. Chang, N. H. Lin, A. L. Yu and C. H. Chen, *Anal. Chem.*, 2008, **80**, 2524-2530.
55. N. Contino, E. Pierson, D. Keifer and M. Jarrold, *Journal of The American Society for Mass Spectrometry*, 2013, **24**, 101-108.
56. M. Gamero-Castano, *The Review of scientific instruments*, 2007, **78**, 043301.
57. U. P. Schlunegger, M. Stoeckli and R. M. Caprioli, *Rapid Communications in Mass Spectrometry*, 1999, **13**, 1792-1796.
58. W. P. Peng, Y. Cai, Y. T. Lee and H. C. Chang, *International Journal of Mass Spectrometry*, 2003, **229**, 67-76.
59. B. M. Prentice and S. A. McLuckey, *Anal. Chem.*, 2012, **84**, 7562-7569.
60. C. Uetrecht, C. Versluis, N. R. Watts, W. H. Roos, G. J. L. Wuite, P. T. Wingfield, A. C. Steven and A. J. R. Heck, *Proceedings of the National Academy of Sciences*, 2008, **105**, 9216-9220.
61. M. Dole, L. L. Mack, R. L. Hines, R. C. Mobley, L. D. Ferguson and M. B. Alice, *The Journal of Chemical Physics*, 1968, **49**, 2240-2249.

62. M. A. Tito, K. Tars, K. Valegard, J. Hajdu and C. V. Robinson, *Journal of the American Chemical Society*, 2000, **122**, 3550-3551.
63. G. K. Shoemaker, E. van Duijn, S. E. Crawford, C. Uetrecht, M. Baclayon, W. H. Roos, G. J. L. Wuite, M. K. Estes, B. V. V. Prasad and A. J. R. Heck, *Mol Cell Proteomics*, 2010, **9**, 1742-1751.
64. J. Snijder, R. J. Rose, D. Veesler, J. E. Johnson and A. J. R. Heck, *Angewandte Chemie International Edition*, 2013, **52**, 4020-4023.
65. G. A. Khitrov and G. F. Strouse, *Journal of the American Chemical Society*, 2003, **125**, 10465-10469.
66. J. K. Navin, M. E. Grass, G. A. Somorjai and A. L. Marsh, *Anal. Chem.*, 2009, **81**, 6295-6299.
67. A. A. Kolomenskii, H. A. Schuessler, V. G. Mikhalevich and A. A. Maznev, *Journal of Applied Physics*, 1998, **84**, 2404-2410.
68. R. F. Wuerker, H. Shelton and R. V. Langmuir, *Journal of Applied Physics*, 1959, **30**, 342-349.
69. L. Ding, M. Sudakov, F. L. Brancia, R. Giles and S. Kumashiro, *J Mass Spectrom*, 2004, **39**, 471-484.
70. I. C. Lu, J. L. Lin, S.-H. Lai and C.-H. Chen, *Anal. Chem.*, 2011, **83**, 8273-8277.
71. R. A. Millikan, *Physical Review (Series I)*, 1911, **32**, 349-397.
72. G. Hars and Z. Tass, *Journal of Applied Physics*, 1995, **77**, 4245-4250.
73. S. Schlemmer, J. Illemann, S. Wellert and D. Gerlich, *Journal of Applied Physics*, 2001, **90**, 5410-5418.
74. S. Schlemmer, S. Wellert, F. Windisch, M. Grimm, S. Barth and D. Gerlich, *Appl Phys A*, 2004, **78**, 629-636.
75. Y. Cai, W. P. Peng, S. J. Kuo, Y. T. Lee and H. C. Chang, *Anal. Chem.*, 2001, **74**, 232-238.
76. Y. Cai, W. P. Peng, S. J. Kuo and H. C. Chang, *International Journal of Mass Spectrometry*, 2002, **214**, 63-73.
77. W.-P. Peng, Y.-C. Yang, C.-W. Lin and H.-C. Chang, *Anal. Chem.*, 2005, **77**, 7084-7089.
78. W.-P. Peng, Y. T. Lee, J. W. Ting and H.-C. Chang, *Review of Scientific Instruments*, 2005, **76**, 023108.
79. A. J. Trevitt, P. J. Wearne and E. J. Bieske, *International Journal of Mass Spectrometry*, 2007, **262**, 241-246.
80. Y. Cai, W. P. Peng, S. J. Kuo, S. Sabu, C. C. Han and H. C. Chang, *Anal. Chem.*, 2002, **74**, 4434-4440.
81. F. Talbot, S. Sciuto and R. Jockusch, *Journal of The American Society for*

Mass Spectrometry, 2013, **24**, 1823-1832.

82. Z. Nie, F. Cui, Y. K. Tzeng, H. C. Chang, M. Chu, H. C. Lin, C. H. Chen, H. H. Lin and A. L. Yu, *Anal. Chem.*, 2007, **79**, 7401-7407.
83. Z. Nie, F. Cui, M. Chu, C. H. Chen, H. C. Chang and Y. Cai, *International Journal of Mass Spectrometry*, 2008, **270**, 8-15.
84. S.-W. Chou, G.-R. Shiu, H.-C. Chang and W.-P. Peng, *Journal of The American Society for Mass Spectrometry*, 2012, **23**, 1855-1864.
85. C. Xiong, G. Xu, X. Zhou, J. Wang, Y. Tang, R. Chen, W. P. Peng, H. C. Chang and Z. Nie, *Analyst*, 2012, **137**, 1199-1204.
86. Z. Zhu, C. Xiong, G. Xu, H. Liu, X. Zhou, R. Chen, W.-P. Peng and Z. Nie, *Analyst*, 2011, **136**, 1305-1309.
87. H. C. Lin, H. H. Lin, C. Y. Kao, A. L. Yu, W. P. Peng and C. H. Chen, *Angew Chem Int Edit*, 2010, **49**, 3460-3464.
88. W.-P. Peng, C.-H. Chen and A. L. Yu, *G.I.T. Laboratory Journal*, 2010, **9-10**, 32-35.
89. C. Q. Xiong, X. Y. Zhou, R. Chen, Y. M. Zhang, W. P. Peng, Z. X. Nie, H. C. Chang, H. W. Liu and Y. Chen, *Anal. Chem.*, 2011, **83**, 5400-5406.
90. C. Xiong, X. Zhou, J. Wang, N. Zhang, W.-P. Peng, H.-C. Chang and Z. Nie, *Anal. Chem.*, 2013, **85**, 4370-4375.
91. C. H. Chen, J. L. Lin, M. L. Chu and C. H. Chen, *Anal. Chem.*, 2010, **82**, 10125-10128.
92. K. G. Standing, *International Journal of Mass Spectrometry*, 2000, **200**, 597-610.
93. N. R. Daly, *Review of Scientific Instruments*, 1960, **31**, 264-267.
94. G. C. Hilton, J. M. Martinis, D. A. Wollman, K. D. Irwin, L. L. Dulcie, D. Gerber, P. M. Gillevet and D. Twerenbold, *Nature*, 1998, **391**, 672-675.
95. M. Frank, S. E. Labov, G. Westmacott and W. H. Benner, *Mass Spectrometry Reviews*, 1999, **18**, 155-186.
96. M. Frank, C. A. Mears, S. E. Labov, W. H. Benner, D. Horn, J. M. Jaklevic and A. T. Barfknecht, *Rapid Communications in Mass Spectrometry*, 1996, **10**, 1946-1950.
97. R. J. Wenzel, U. Matter, L. Schultheis and R. Zenobi, *Anal. Chem.*, 2005, **77**, 4329-4337.
98. A. A. Aksenov and M. E. Bier, *Journal of the American Society for Mass Spectrometry*, 2008, **19**, 219-230.
99. M. E. Bier, *Flexible Package Conf. of the Society of Plastics Engineers*, 2008, Feb. 24-27th.
100. F. Bouyjou, H. Tap-Beteille, J. Sauvaud, R. Molina and C. Aoustin, Integration

of a 16-channel low power cmos instrumentation chain for electron and charged particle detection in astrophysics, 2010.

101. H. Shelton, C. D. Hendricks and R. F. Wuerker, *Journal of Applied Physics*, 1960, **31**, 1243-1246.
102. D. Z. Keifer, E. E. Pierson, J. A. Hogan, G. J. Bedwell, P. E. Prevelige and M. F. Jarrold, *Rapid Communications in Mass Spectrometry*, 2014, **28**, 483-488.
103. E. E. Pierson, D. Z. Keifer, L. Selzer, L. S. Lee, N. C. Contino, J. C. Y. Wang, A. Zlotnick and M. F. Jarrold, *Journal of the American Chemical Society*, 2014, **136**, 3536-3541.
104. R. Anumolu, J. A. Gustafson, J. J. Magda, J. Cappello, H. Ghandehari and L. F. Pease, *ACS Nano*, 2011, **5**, 5374-5382.
105. S. Guha, L. F. Pease Iii, K. A. Brorson, M. J. Tarlov and M. R. Zachariah, *Journal of Virological Methods*, 2011, **178**, 201-208.
106. K. D. Cole, L. F. Pease Iii, D.-H. Tsai, T. Singh, S. Lute, K. A. Brorson and L. Wang, *Journal of Chromatography A*, 2009, **1216**, 5715-5722.
107. A. A. Rostom and C. V. Robinson, *Journal of the American Chemical Society*, 1999, **121**, 4718-4719.
108. C. Uetrecht, C. Versluis, N. R. Watts, P. T. Wingfield, A. C. Steven and A. J. R. Heck, *Angewandte Chemie International Edition*, 2008, **47**, 6247-6251.
109. S. Rosati, R. J. Rose, N. J. Thompson, E. van Duijn, E. Damoc, E. Denisov, A. Makarov and A. J. R. Heck, *Angewandte Chemie International Edition*, 2012, **51**, 12992-12996.
110. A. Makarov, E. Denisov, A. Kholomeev, W. Balschun, O. Lange, K. Strupat and S. Horning, *Anal. Chem.*, 2006, **78**, 2113-2120.
111. A. Makarov, *Anal. Chem.*, 2000, **72**, 1156-1162.
112. M. Hardman and A. A. Makarov, *Anal. Chem.*, 2003, **75**, 1699-1705.
113. A. R. McKay, B. T. Ruotolo, L. L. Ilag and C. V. Robinson, *Journal of the American Chemical Society*, 2006, **128**, 11433-11442.
114. M. Mann, C. K. Meng and J. B. Fenn, *Anal. Chem.*, 1989, **61**, 1702-1708.
115. R. Winkler, *Rapid Communications in Mass Spectrometry*, 2010, **24**, 285-294.
116. J. J. Hagen and C. A. Monnig, *Anal. Chem.*, 1994, **66**, 1877-1883.
117. B. Reinhold and V. Reinhold, *Journal of the American Society for Mass Spectrometry*, 1992, **3**, 207-215.
118. H. Zheng, P. C. Ojha, S. McClean, N. D. Black, J. G. Hughes and C. Shaw, *Rapid Communications in Mass Spectrometry*, 2003, **17**, 429-436.
119. A. Almudaris, D. Ashton, C. Beddell, D. Cooper, S. Craig and R. Oliver, *European Journal of Mass Spectrometry*, 1996, **2**, 57-67.
120. B. van Breukelen, A. Barendregt, A. J. R. Heck and R. H. H. van den Heuvel,

Rapid Communications in Mass Spectrometry, 2006, **20**, 2490-2496.

121. J. E. Bruce, X. Cheng, R. Bakhtiar, Q. Wu, S. A. Hofstadler, G. A. Anderson and R. D. Smith, *Journal of the American Chemical Society*, 1994, **116**, 7839-7847.
122. X. Cheng, D. G. Camp, Q. Wu, R. Bakhtiar, D. L. Springer, B. J. Morris, J. E. Bruce, G. A. Anderson, C. G. Edmonds and R. D. Smith, *Nucleic Acids Research*, 1996, **24**, 2183-2189.
123. F. Stengel, A. J. Baldwin, M. F. Bush, G. R. Hilton, H. Lioe, E. Basha, N. Jaya, E. Vierling and J. L. P. Benesch, *Chem Biol*, 2012, **19**, 599-607.
124. G. N. Sivalingam, J. Yan, H. Sahota and K. Thalassinos, *International Journal of Mass Spectrometry*, 2013, **345–347**, 54-62.
125. M. Yang, J. M. Dale, W. B. Whitten and J. M. Ramsey, *Anal. Chem.*, 1995, **67**, 1021-1025.
126. J. V. Johnson, R. A. Yost, P. E. Kelley and D. C. Bradford, *Anal. Chem.*, 1990, **62**, 2162-2172.
127. J. V. Olsen, J. C. Schwartz, J. Griep-Raming, M. L. Nielsen, E. Damoc, E. Denisov, O. Lange, P. Remes, D. Taylor, M. Splendore, E. R. Wouters, M. Senko, A. Makarov, M. Mann and S. Horning, *Mol Cell Proteomics*, 2009, **8**, 2759-2769.
128. Y.-F. Hsu, J.-L. Lin, M.-L. Chu and C.-H. Chen, *Analyst*, 2013, **138**, 4823-4829.
129. L. Fornelli, J. Parra, R. Hartmer, C. Stoermer, M. Lubeck and Y. Tsybin, *Anal Bioanal Chem*, 2013, **405**, 8505-8514.
130. H. Koizumi, W. B. Whitten and P. T. A. Reilly, *Journal of the American Society for Mass Spectrometry*, 2008, **19**, 1942-1947.
131. H. Koizumi, X. Wang, W. B. Whitten and P. T. A. Reilly, *Journal of the American Society for Mass Spectrometry*, 2010, **21**, 242-248.
132. J. Lee, H. Chen, T. Liu, C. E. Berkman and P. T. Reilly, *Anal. Chem.*, 2011, **83**, 9406-9412.

Figure Captions:

Figure 1(a) Experimental setup of an ambient desorption CMS which consists an AD ion source, a QIT mass analyzer, and a charge detector. (b) Schematic of ambient desorption process. The microparticles are desorbed by aerodynamic force and inhaled into the mass spectrometer when discontinuous atmospheric interface (DAPI) was open. Reprinted with permission from ref. 90.

Figure 2 A nanomembrane detector. (a) Schematic of the detector coupled to a MALDI-TOF mass spectrometer. (b) Detailed illustration of the operation principle of the detector. (c) Schematic of the detector configuration, consisting of a trilayer made of Al/Si3N4/Al, an extraction gate, MCP, and an anode. The right inset is the MALDI TOF mass spectrum of IgM with a nanomembrane detector (a) IgM mass spectrum. Inset: histogram of IgM. (b) The FWHM mass resolution of the detector. Reprinted from ref. 45 and ref. 46 with permission.

Figure 3 The gated electrostatic ion trap. Trapping plates on the left and right sides of the detector module define the potential field that forces ions to cycle back and forth through the detector tube. A support arm, attached to the bottom of the detector block, holds the detector assembly rigidly to minimize vibrations and shields an internal FET from rf noise. Reprinted with permission from ref. 40.

Figure 4 Induction charge detector with multiple sensing stages. Reprinted with permission from ref. 56.

Figure 5 Schematic of the different components of the electrospray–differential mobility analysis (ES–DMA) system. Reprinted with permission from ref. 43.

Figure 6 (a) Mass spectrum of GroEL. (b) CID mass spectrum of MS2 virus capsid ions. Reprinted from ref. 107 and ref. 62 with permission.

Figure 7 Schematic layout of the modified Q-TOF 1 instrument (Micromass, U.K.). Items in dark blue are modifications relative to the standard Q-TOF 1 configuration. Reprinted with permission from ref. 30.

Figure 8 The assembly of HK97 capsids analyzed with native ESI-MS. a) Assembly and maturation pathway of HK97. b) Free capsomers with penton signal in blue and hexon signal in red. c) Intact Prohead-1 particle. Reprinted with permission from ref.

64.

Figure 9 Schematic of the modified Exactive Plus instrument with HCD option. Reprinted with permission from ref. 31.

Figure 10 (a) Deconvolution of the cytochrome c (M = 12360) mass spectrum. The theoretical positions of the first side peaks are marked by dark triangles. (b) "Zoom" expansion of the spectrum in (a) for the mass range between 10 000 and 14 000. Reprinted with permission from ref. 114.

Figure 11 (a) Mass spectrum of HBV ions. Analysis of HBV capsids (b) T = 3 ions, (c) T = 4 ions, and (d) mixture of T = 3 and T = 4 ions in the overlapping m/z region. The insert shows the selected m/z peaks for the analysis in part d. Reprinted with permission from ref. 18.

Figure 12 AutoMass analysis of CID tandem mass spectra of HBV capsids at an accelerating voltage of 400 V. (a) CID mass spectrum of T = 3 ions, (b) the AutoMass analysis of (a), (c) CID mass spectrum of T = 4 ions, (d) the AutoMass analysis of (c). N0 denotes the number of proteins in the oligomers. Reprinted with permission from ref. 19.

Figure 13 Massign assignment of subunit complexes 5, 2, 3, and 4 are shown in (A), (B), (C), and (D) respectively. Final assignment for all 4 complexes to the series is shown in (E). Reprinted with permission from ref. 20.

Figure 1

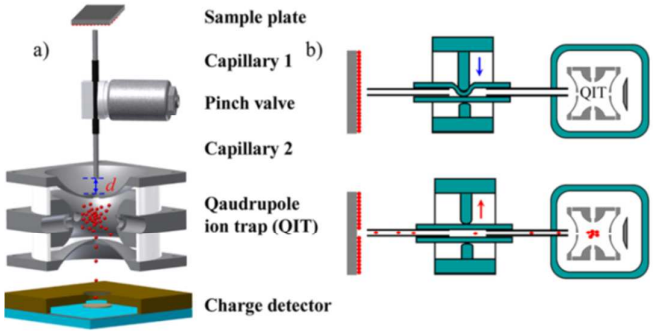

Figure 2

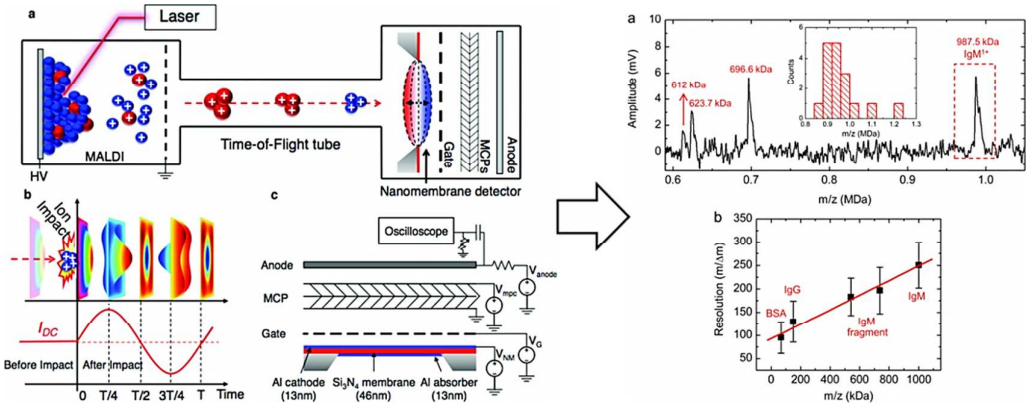

Figure 3

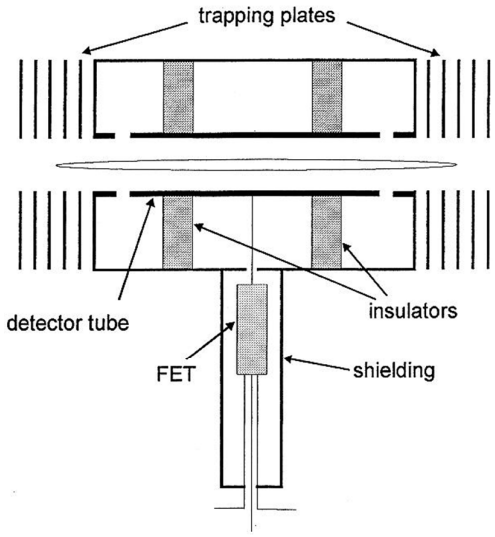

Figure 4

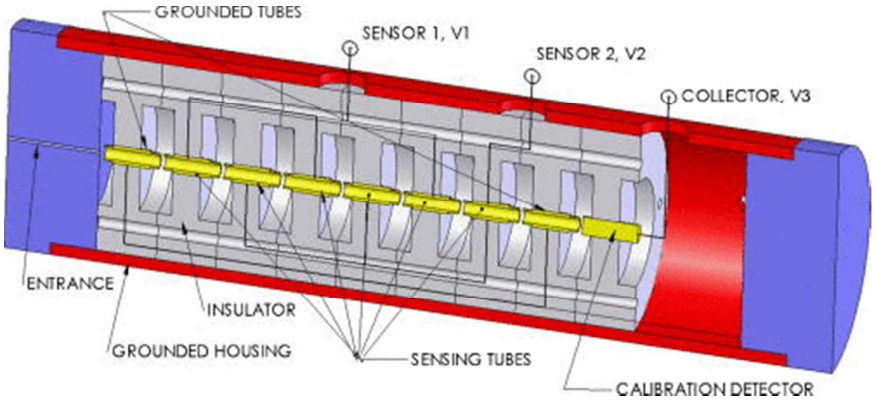

Figure 5

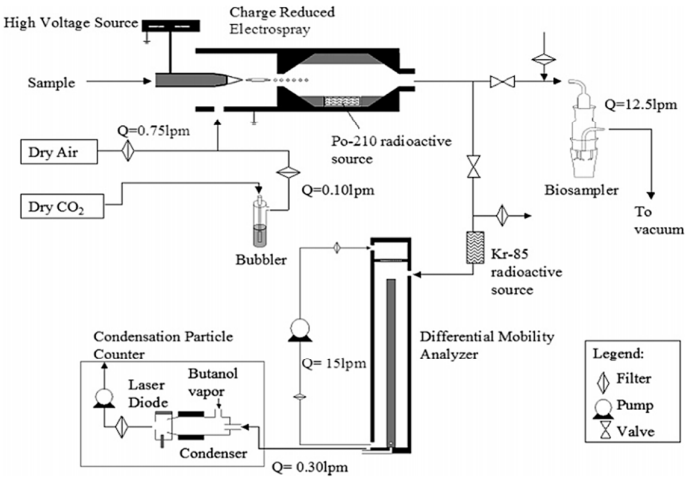

Figure 6

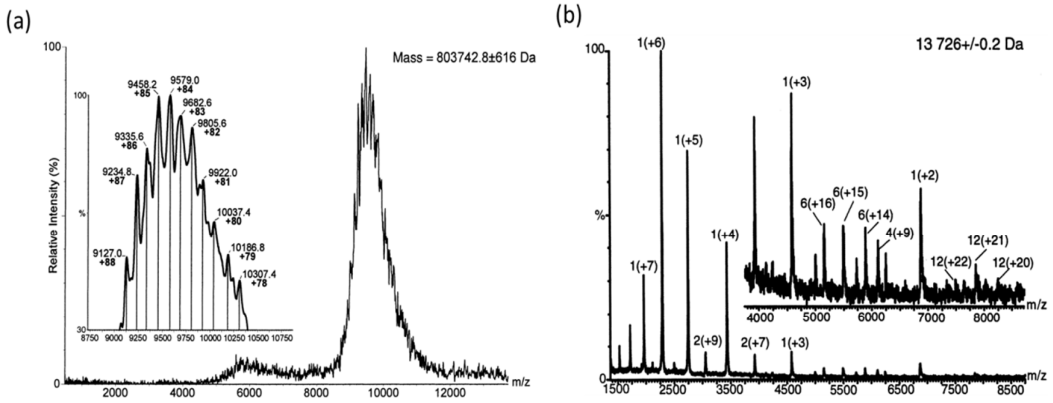

Figure 7

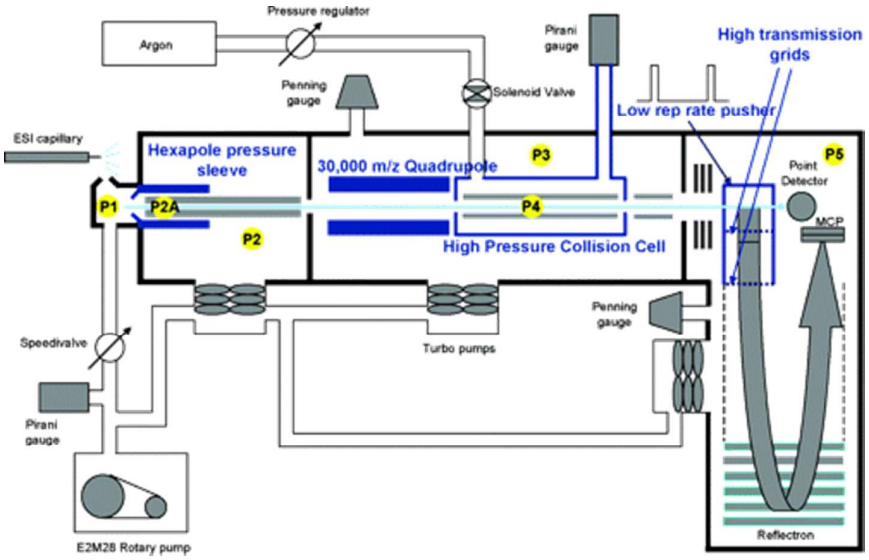

Figure 8

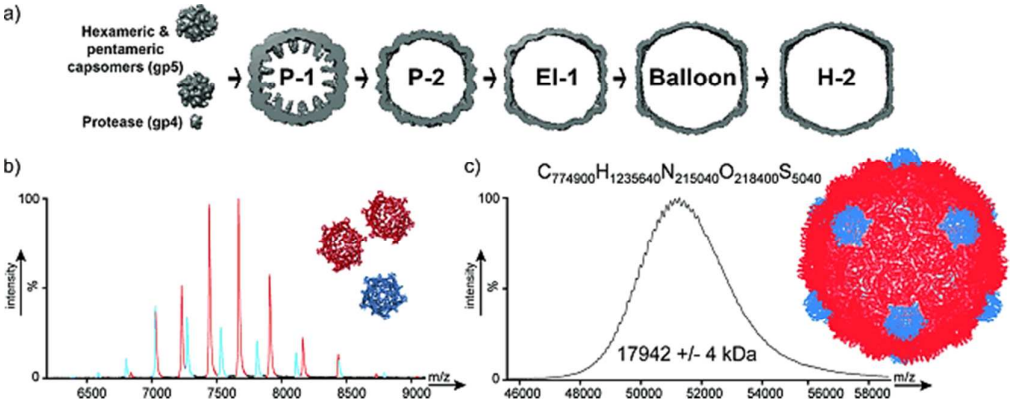

Figure 9

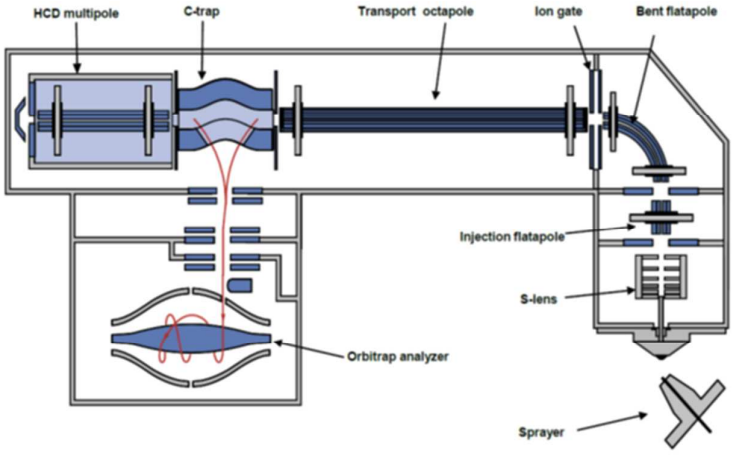

Figure 10

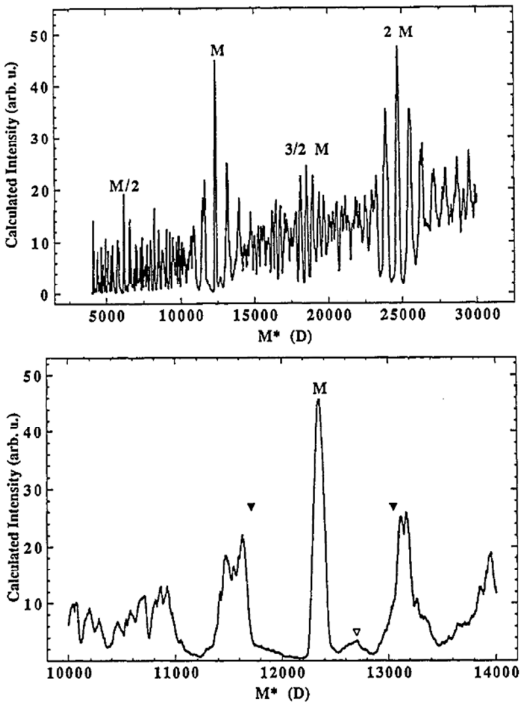

Figure 11

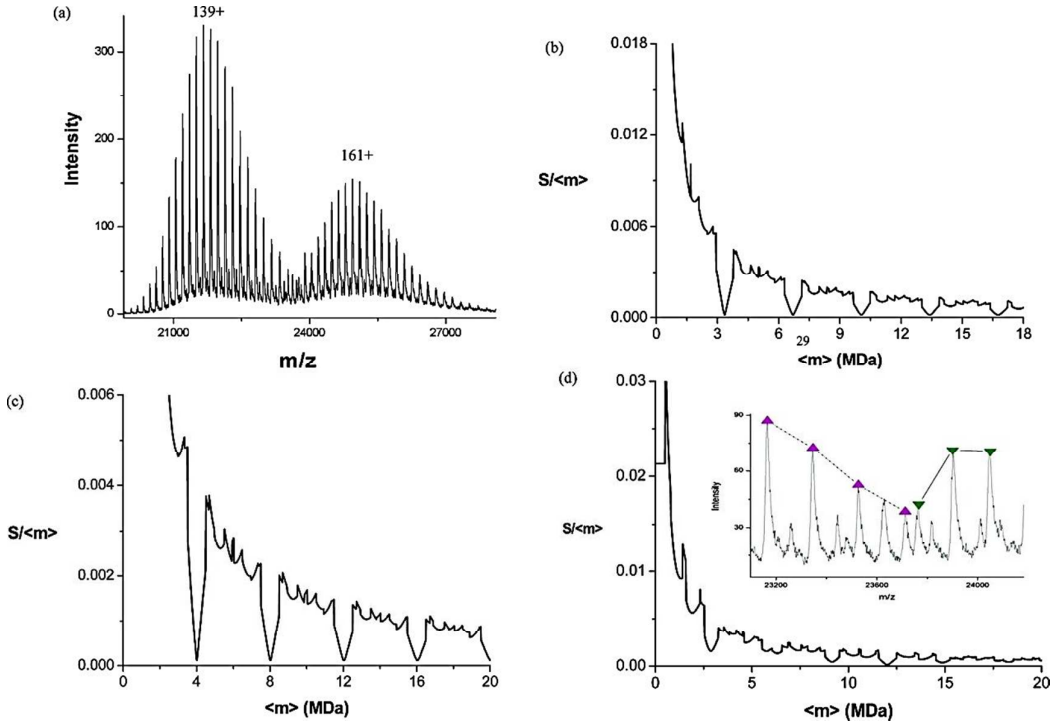

Figure 12

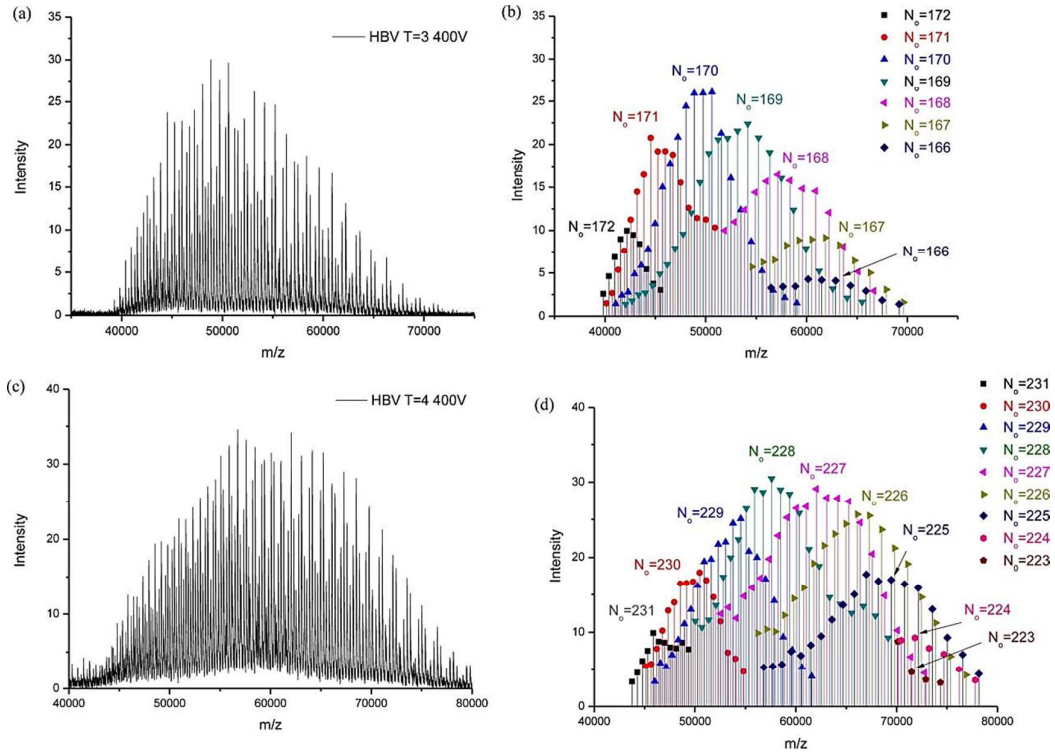

Figure 13

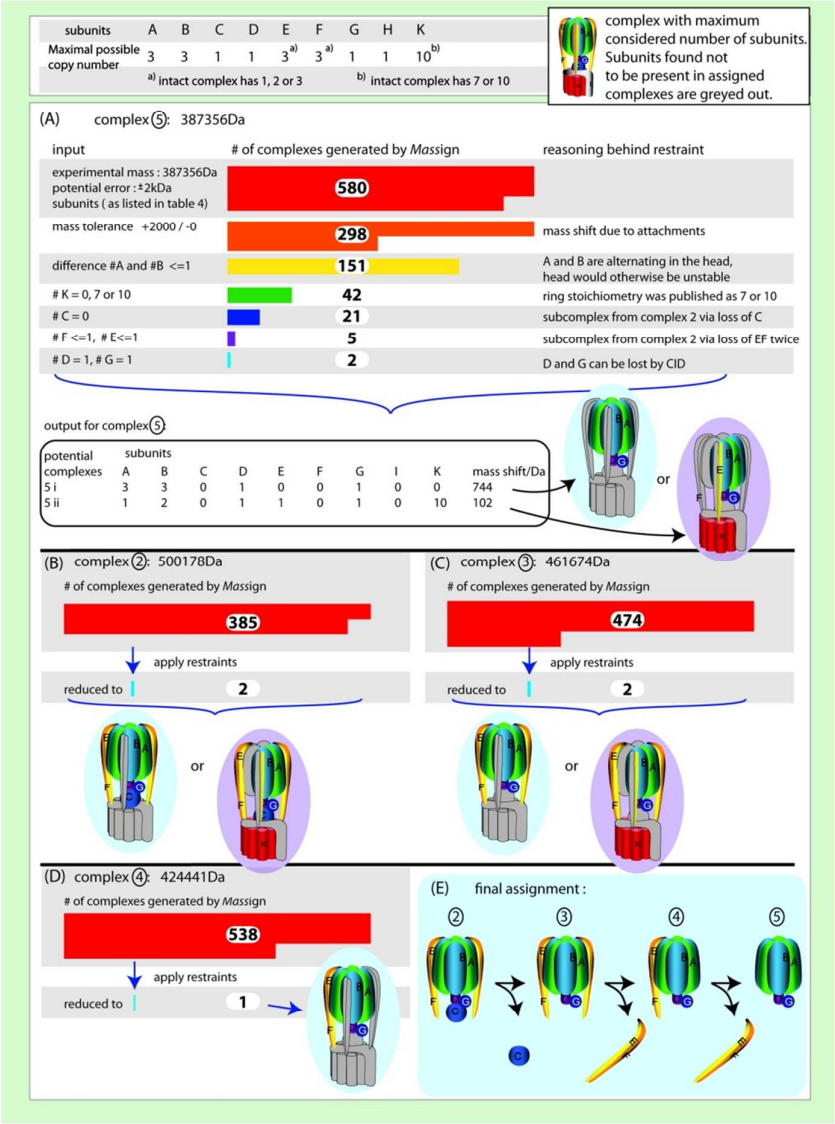

Table 1. Comparison of physical mass spectrometric techniques available for large biomolecules and bioparticles

Mass spectrometry techniques	Analytes	Analyzer/ detector	Particle Size (nm)	Particle mass (Da)	Mass resolution (m/Δm)	Mass accuracy	Refs.
Quadrupole ion trap mass spectrometry	Micro particles, nanodiamond, nanoparticles, bacteria/ viruses/cells	secondary electron	<10	$<10^6$	$10\text{-}10^3$	-	57,69
		light scattering	$10\text{-}10^3$	$<10^{12}$	$10\text{-}10^4$	1%	12, 28, 53, 68, 72-75, 77-79
		laser induced fluorescence	$10\text{-}10^2$	$<10^5$	-	-	5, 58, 80
		charge detector	$10\text{-}10^4$	$<10^{16}$	$\sim10^2$	1%	4, 27, 54, 82-85, 87-90
Linear ion trap mass spectrometry	protein, protein complexes, organic compounds	secondary electron, charge detector	$<10^1$	$<10^6$	$\sim10^2$	-	70, 130, 131
Time-of-flight (TOF) mass spectrometry	protein, protein complexes, organic compounds, polymer, nanoparticles	secondary electron, cryogenic detector, nanomembrane, charge detector	$10\text{-}10^2$	$<10^6$	$10\text{-}10^3$	1%	23, 24, 45-48, 95, 96
Charge detection mass spectrometry	micro particles, nanoparticles, protein, protein complex, viruses	charge detector, linear array, recirculating trap	$10\text{-}10^4$	$<10^{12}$	$10\text{-}10^2$	-	40, 55, 56, 102
Differential mobility mass Spectrometry (DMA)	nanoparticles, microparticles, bacteria/ viruses	DMA	$10\text{-}10^4$	$10^9\text{-}10^{12}$	$10\text{-}10^2$	-	43, 44, 104-106
Quadrupole orthogonal time-of-flight mass spectrometry	Protein, protein complexes, virus capsids	TOF, secondary electron	$10\text{-}10^2$	$<10^6$	$10\text{-}10^3$	0.1%	30, 60, 62-64, 108, 132
Orbitrap mass spectrometry	antibodies, viral cell, protein, protein Complexes	orbitrap	$10\text{-}10^2$	$<10^6$	$\sim10^4$	0.001%	31, 32, 41, 109